

## Endothelial monocyte activating polypeptide-II induced gene expression changes in endothelial cells

Anita T. Tandle<sup>a</sup>, Chiara Mazzanti<sup>a</sup>, H. Richard Alexander<sup>a</sup>,  
David D. Roberts<sup>b</sup>, Steven K. Libutti<sup>a,\*</sup>

<sup>a</sup>*Surgery Branch, Center for Cancer Research, National Cancer Institute, Bethesda, MD 20892, USA*

<sup>b</sup>*Laboratory of Pathology, Center for Cancer Research, National Cancer Institute, Bethesda, MD 20892, USA*

Received 22 November 2004; accepted 16 January 2005

### Abstract

In the current study we used microarray (MA) analysis to examine gene expression changes in human umbilical vein endothelial cells (HUVEC) exposed to the tumor-derived cytokine, endothelial monocyte-activating polypeptide-II (EMAP-II). HUVEC treated with EMAP-II for 0.5, 1, 2, 4 and 8 h, were analyzed using 10K cDNA arrays. Our results demonstrated that changes in gene expression of <0.5 and >2 fold were seen for 69 genes and the majority of gene changes occurred early. Validation of MA analysis for 10 genes by real time RT-PCR, demonstrated the gene changes to be consistent and specific to HUVEC when compared to human fibroblasts treated with EMAP-II. Among these genes, downregulated in ovarian cancer 1 (DOC1) gene was studied further because of its possible role in EMAP-II induced cytoskeletal remodeling. DOC1 expression was silenced using small interfering RNA. SiRNA to DOC1 completely abolished EMAP-II stimulated gene expression of DOC1. Silencing of DOC1 gene expression reversed the modulatory effect of EMAP-II on 4 other genes, suggesting that DOC1 might play a role in mediating some of the effects of EMAP-II on endothelial cells.

Published by Elsevier Ltd.

*Keywords:* DOC1; EMAP-II; Endothelial cells; Microarray analysis; SiRNA

### 1. Introduction

The proinflammatory cytokine endothelial monocyte activating polypeptide-II (EMAP-II) was first detected in the supernatants of murine tumor cells by virtue of its ability to stimulate endothelial-dependent coagulation in vitro [1]. The mature 23 kDa form of EMAP-II, for which the biological activities have been described, is synthesized as a precursor protein lacking a conventional secretion signal peptide [2]. It has been shown that caspase-7 cleaves and releases mature EMAP-II in vitro

from proEMAP-II [3]. Hypoxia is also a potent inducer of release of biologically active EMAP-II [4].

Purified EMAP-II has pleiotropic effects on endothelial cells (ECs), monocytes, and neutrophils. In addition to the induction of tissue factor-dependent coagulation on ECs and monocytes, EMAP-II up-regulates endothelial E- and P-selectin expression and stimulates the release of von Willebrand factor. It acts as a chemoattractant for neutrophils and monocytes and induces release of myeloperoxidase activity from neutrophils [2]. It inhibits EC proliferation by binding to  $\alpha$ -adenosine triphosphate synthase [5]. EMAP-II can also inhibit neovascularization, in both matrigel and corneal angiogenesis models [6,7].

The effects of EMAP-II on tumor growth are complex. EMAP-II abrogates tumor growth by induction of EC

\* Corresponding author at Surgery Branch, Center for Cancer Research, National Cancer Institute, 10 Center Drive, Building 10, Room 4W-5940, Bethesda, MD 20892-1201, USA. Tel.: +1 301 496 5049; fax: +1 301 402 1788.

*E-mail address:* libuttis@mail.nih.gov (S.K. Libutti).

apoptosis in vivo [3,6–8]. It also sensitizes tumors to the effect of tumor necrosis factor (TNF)- $\alpha$  [9,10]. It has been shown that EMAP-II upregulates TNF-receptor 1 expression by ECs both in vitro and in vivo [7]. The induction of TNF receptor 1 expression may be the mechanism by which EMAP-II sensitizes tumor endothelium to the effects of TNF leading to hemorrhagic necrosis.

The regulation of gene expression is a fundamental step in cellular physiology. With previous molecular techniques, regulation of gene expression could only be studied on a small number of genes at a time. Newly developed molecular genetic and computational technology has enabled us to analyze differential gene expression profiles of thousands of genes collectively in response to a single stimulus. DNA microarray (MA) technology represents a powerful tool for rapid, comprehensive, and quantitative analysis of gene expression profiles of normal/disease states and developmental processes [11–13]. This approach is ideally suited for studying the pattern of gene expression in ECs induced by various experimental conditions [14].

EMAP-II is a multifunctional protein, and there has been intense study of its effects on various cell types in vitro and in vivo [2,6,7,9,10]. However, the molecular mechanisms behind its action are not known. In the current study, we have used cDNA MA to examine changes in the expression profile of various genes in human umbilical vein endothelial cells (HUVEC) in response to EMAP-II treatment, in order to gain a better understanding of the specific pathways involved in the activity of EMAP-II on ECs.

## 2. Results

### 2.1. EMAP-II specifically inhibits HUVEC cell proliferation

HUVEC and human fibroblast cells were treated with EMAP-II for 2 h, 4 h, 1 day, 3 days and 5 days. The cells treated with EMAP-II elution buffer (as given in the Section 4), endostatin and 5-fluorouracil (5-FU) were used as controls. The results of the proliferation assay are shown in Fig. 1. Treatment with 10  $\mu$ g of EMAP-II inhibited HUVEC proliferation in a time-dependent manner compared to non-treated controls (Fig. 1a). However, EMAP-II did not inhibit proliferation of human fibroblasts (Fig. 1b). Thus, the inhibitory activity of EMAP-II on cell proliferation appears to be specific for ECs when compared to fibroblasts.

### 2.2. EMAP-II induces specific gene expression changes in HUVEC

HUVEC cells treated with EMAP-II as described in the section 4 were studied using cDNA MA analysis. Of

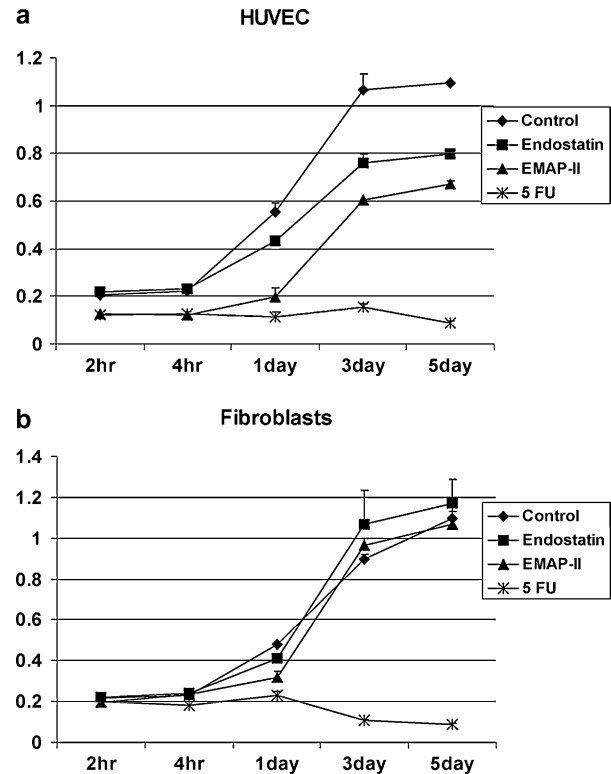


Fig. 1. Cell proliferation assay. HUVEC (a) or human fibroblasts (b) (2000/well) were plated and treated with carrier control, 5-FU (50  $\mu$ g/ml) and Endostatin (10  $\mu$ g/ml) as a positive control and 10  $\mu$ g/ml EMAP-II for 2 h, 4 h, 1 day, 3 days and 5 days. Inhibition of cell proliferation was tested using WST reagent and viable cell number measured at 440 nm. The line graphs were plotted using treatment time on the X axis against the OD readings on the Y axis. EMAP-II specifically inhibited proliferation of HUVEC (a) but not fibroblasts (b).

the 10,000 genes on the MA, 8382 genes were examined after correction for signal intensity and signal to background ratio at every spot. To examine overall changes in gene expression at different time points, scatter plots of basal expression (0 h) vs. expression at 0.5, 1, 2, 4 and 8 h were drawn on 8382 genes using BRB Array Tools (Fig. 2). The lines indicate 1:2 or 2:1 ratios between basal expression and expression at each time point. We observed the maximum number of genes changing their expression patterns between 0.5 and 2 h.

We observed changes in 69 genes using a twofold cutoff threshold ( $\log$  ratio  $\geq 2$  or  $\leq 0.5$ ). The 69 genes, arranged in different categories according to their function, are shown in Table 1 with gene ID (used from Incyte Genomics, Inc.) and fold changes (linear scale) in gene expression at different time points compared to baseline.

Of the 69 genes, which demonstrated changes in response to EMAP-II treatment of HUVEC in our study, 18 genes have previously been reported to be modulated in EC including HUVEC when exposed to stimuli other than EMAP-II (Table 2). We observed

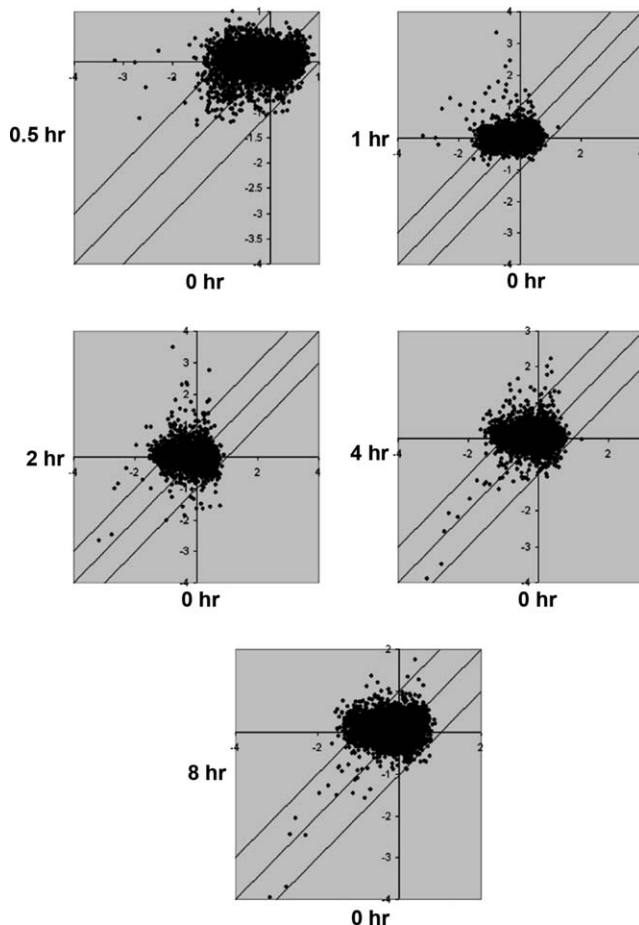


Fig. 2. Gene expression profile. Scatter plots of signals from microarray analysis of HUVEC treated with EMAP-II. Each dot indicates a ratio between Cy5/Cy3 signals. Scatter plots are drawn on 8382 genes using BRB Array Tools comparing baseline expression (0 h) to the expression at 0.5 h, 1 h, 2 h, 4 h and 8 h. The two lines at the periphery indicate 1:2 or 2:1 ratios between basal expression and expression at each time point.

upregulation in 63/69 and downregulation in 6/69 genes. 28 (40.5%) genes showed  $\geq 2$  to 3 fold changes, 24 (35%) genes showed  $\geq 3$  to 5 fold with 17 (24.5%) genes with  $> 5$  fold changes. The highest (18.9 fold) upregulation was seen in the gene HEPERUD1; however, so far no function has been assigned to this gene. Of the 69 genes, 64 genes showed changes within 0.5–2 h of treatment.

We selected 10 of the 69 genes to validate the gene changes observed on MA analysis using real time RT-PCR; ADM, DOC1, FOS, ICAM1, ID1, ID2, KIT, KLF4, SOCS3, and TNFAIP3. The genes were selected depending on their function and expression pattern. The 10 genes are involved in various functions; cell proliferation/differentiation, cell death, adhesion, signal transduction, oncogenesis and are either upregulated (high to moderate) or down regulated (Table 1). The log<sub>2</sub> gene expression values of the 10 genes obtained on MA analysis are plotted as a line graph in order to observe the pattern of gene changes over time (Fig. 3). Genes,

such as DOC1, FOS, ID1, ID2, KLF4, SOCS3 and TNFAIP3 are upregulated by 1–2 h and then the expression starts to return to baseline. By contrast ICAM1 slowly goes up and remains at steady state level even at the 8 h time point. The expression pattern for ADM and KIT differs in that it is maximally down-regulated by 2 h and then comes back to its basal level by 8 h.

For these same 10 genes, the gene expression changes were validated using real time RT-PCR (Fig. 4a,b). Real time RT-PCR validated the expression pattern for the genes, ADM, DOC1, ID1, KIT, SOCS3, TNFAIP3 and ICAM1. Although KLF4 showed up-regulation, the pattern was slightly different and the gene changes for FOS and ID2 genes could not be confirmed by RT-PCR.

We also checked whether the gene changes observed in HUVEC on EMAP-II stimulation were specific to ECs. To study this, total RNA from EMAP-II treated fibroblasts was subjected to real time RT-PCR (Fig. 4c,d). As seen in Fig. 4c,d, there was virtually no changes in the expression pattern for genes, ID1, ID2, KLF4 and SOCS3 in fibroblasts, although these genes were upregulated in HUVEC. The FOS gene showed similar changes both in HUVEC and fibroblasts. Although the genes DOC1, TNFAIP3 and ICAM1 were upregulated in fibroblasts, the pattern of change was different as compared to HUVEC. The fibroblasts showed upregulation of the ADM and KIT oncogene in contrast to downregulation of both the genes in HUVEC. Thus, the results indicate that the gene changes seen in EMAP-II treated HUVEC are different than the effects seen in fibroblasts.

### 2.3. DOC1 small interfering RNA (SiRNA) reverses the effect of EMAP-II on DOC1 expression

We wanted to examine if the inhibition of the expression of any single gene could affect the levels of expression of any of the other genes tested after EMAP-II stimulation. Such a result might imply the presence of a regulatory pathway. For this purpose, we selected the DOC1 gene as it might play a role in EMAP-II induced cytoskeleton organization in ECs [15]. HUVEC transfected with pSiRNA-Neo-Control and pSiRNA-Neo-DOC1 SiRNA, were stimulated with EMAP-II for 0 h, 1 h, 2 h and 4 h and subjected to real time RT-PCR. Control SiRNA did not show any effect on gene expression, as a similar pattern of gene expression was seen with and without pSiRNA-Neo-Control in EMAP-II stimulated HUVEC (Figs. 4a and 5a). SiRNA to the DOC1 gene completely abolished EMAP-II stimulated gene expression of DOC1, compared to HUVEC treated with control SiRNA (Fig. 5a). To determine if DOC1 regulated the expression of any of the other genes modulated by EMAP-II, we performed RT-PCR for

Table 1  
EMAP-II induced gene expression changes in endothelial cells

Pathways	Genes	Gene ID	0.5 h	1 h	2 h	4 h	8 h
Cell cycle	CCNG2	NM_004354	0.75	1.1	1.84	0.67	0.80
	NEDD9	NM_182966	2.0	3.1	2.7	1.0	1.3
Proliferation/ differentiation	DUSP5	NM_004419	1.3	2.7	1.4	1.0	0.76
	FOS	V01512	9.0	9.3	1.4	0.59	0.57
	ID1	NM_181353	1.2	2.4	0.85	0.54	0.47
	ID2	NM_002166	3.0	8	4.9	1.2	1.4
	KLF4	NM_004235	1.8	4.9	2.0	1.4	1.3
	PLAB	NM_004864	1.0	1.0	0.45	0.71	0.66
DNA repair	UNG2	NM_021147	6.7	6.7	1.2	0.60	0.51
Cell death	BIRC3	NM_182962	0.93	1.42	2.5	1.3	1.2
	TNFAIP3	NM_006290	0.7	1.67	2.8	1.3	0.92
Cytoskeleton/ adhesion	ICAM1	NM_000201	1.2	1.4	2.6	3.5	3.3
EC/vascular function	ADM	NM_001124	1.0	0.78	0.24	0.61	1.0
	EDF1	NM_003792	1.1	1.7	2.7	3.1	2.9
	EDN1	NM_001955	1.4	1.6	0.35	1.0	1.4
	SCYE1	NM_004757	1.4	0.9	4.8	1.1	0.90
Oncogenes	KIT	NM_000222	0.93	0.72	0.27	0.43	0.88
	PIM2	NM_006875	0.85	1.4	2.5	1.5	0.78
Inflammation/ immune response	CXCL1	NM_001511	1.5	2.1	5.5	3.5	4.1
	CXCL3	NM_002090	0	1.3	4.1	2.1	1.5
Signal transduction	GEM	NM_005261	1.3	3.3	1.9	0.97	0.95
	MADH7	NM_005904	0.83	4.3	0.85	0.62	0.77
	PDE8A	NM_002605	1.0	1.5	2.3	2.6	2.6
	SEL1L	NM_005065	0.90	1.2	2.2	2.2	2.1
	SOCS3	NM_003955	1.4	3.4	0.87	0	0.88
Transcriptional regulators/TF	ATF3	NM_001674	4.1	10.9	3.2	1.3	1.4
	EGR1	NM_001964	3.1	4.0	0.82	0	0.59
Miscellaneous	EGR2	NM_000399	3.9	5.1	2.0	1.1	1.0
	HES1	NM_005524	1.82	5.4	0	0.70	0.62
	HEY1	NM_012258	1.6	5.8	1.6	0.82	0.79
	JUN	NM_002228	0.78	0.91	0.41	0.66	0.59
	SMARCA5	NM_003601	1.1	0.85	0.53	0.71	0.99
	TIEG	AF050110	1.7	3.7	0.45	1.2	1.0
	ZNF267	NM_003414	0.82	1.8	0.90	0.70	0.86
	C8FW	NM_025195	2.3	3.7	1.3	2.4	2.6
	CYBA	NM_000101	0.47	0.33	0.29	0.44	0.39
	EDEM1	NM_014674	0.94	1.2	2.0	2.2	1.2
	EIF2AK3	NM_004836	0.97	1.7	2.6	1.3	0.66
	ERP70	NM_004911	0.75	0.86	1.2	1.6	1.4
	HSPA5	NM_005347	1.2	1.6	2.5	3.6	2.5
	KIAA0062	D31887	0.88	1.2	2.1	2.8	1.2
	MARS	NM_004990	1.5	6.5	6.6	1.6	1.1
	PDE4B	NM_002600	2.7	2.0	0.70	1.2	1.3
	PIGA	NM_002641	1.1	2.0	3.4	2.6	1.1
	PTGS2	D28235	5.6	11.4	3.7	1.0	0.87
	RNASE4	NM_001145	0.69	0.72	1.3	1.7	1.7
	SERPINB2	NM_002575	0.99	1.4	3.2	4.7	2.1
	SLC21A3	NM_005075	0.98	2.0	4.5	4.3	3.6
	SLC30A1	NM_021194	1.2	2.3	3.2	2.0	1.5
	TRA1	NM_003299	1.8	6.7	6.3	1.0	0
VARS2	NM_006295	0.68	0.60	0.31	0.51	0.48	
FLJ20277	NM_017739	1.1	1.5	2.3	2.2	2.6	
LCN1	L14927	1.2	0.99	0.40	0.92	1.22	
MT2A	NM_175617	0.88	1.2	1.1	1.1	1.2	
STARD4	NM_139164	0.77	1.4	2.1	1.3	0.75	
Unknown	ARMET	NM_006010	2.5	2.7	4.1	4.9	1.9
	C21orf4	NM_006134	0.87	0.97	2.0	3.3	1.5

Table 1 (continued)

Pathways	Genes	Gene ID	0.5 h	1 h	2 h	4 h	8 h
	DEPP	NM_007021	2.1	1.2	0.47	1.9	2.1
	DOC1	NM_014890	2.2	5.9	5.2	1.1	1.5
	HERPUD1	NM_014685	3.3	17.0	18.9	2.3	0.92
	HMOX1	Z82244	0.96	1.1	1.3	1.2	1.0
	LOC11606	L14927	0.83	1.0	1.7	1.0	0.57

The table groups genes that were modulated in HUVEC stimulated by EMAP-II into different categories according to their gene function. The gene ID was obtained from Incyte Genomics Inc. The fold changes in gene expression at different time points 0.5 h, 1 h, 2 h, 4 h and 8 h over the basal expression (0 h) are shown. The table shows 62 genes out of 69, as 7 genes were totally unknown with no information available. HUVEC, human umbilical vein endothelial cells; EMAP-II, endothelial monocyte activating polypeptide II; EC, endothelial cell; TF, transcription factor.

ADM, FOS, ICAM1, ID1, ID2, KIT, KLF4, SOCS3 and TNFAIP3 genes in control SiRNA or DOC1 SiRNA treated and EMAP-II stimulated HUVEC (Fig. 5b–j). Silencing of DOC1 gene expression effectively abrogated the effect of EMAP-II on ADM, KLF-4, SOCS3 and TNFAIP3 gene expression (Fig. 5g–j). However, it had little effect on the modulation of FOS, ICAM1, ID1, KIT genes and no effect on ID2 gene (Fig. 5b–f).

### 3. Discussion

The analysis of gene expression using DNA microarrays is having a tremendous impact on a variety of scientific disciplines. The MA expression patterning can

help us to understand molecular pathways at the cellular level, and may aid us in the diagnosis, prognosis and classification of human diseases [16]. We applied this powerful tool to study the effect of EMAP-II on ECs. Although several studies have described the phenotypic changes in ECs resulting from treatment with EMAP-II, there is very little information available about the genes involved in the response of ECs to EMAP-II. Therefore, in the current study, we examined the changes in the gene expression profile of HUVEC after treatment with recombinant human EMAP-II.

We used a human 10K cDNA MA to identify genes induced by the stimulation of HUVEC with EMAP-II. This analysis showed modulation of 69 genes with a 2 fold cutoff threshold, as indicated in Table 1. This included several genes that have been previously

Table 2  
Gene changes in endothelial cells: published reports

Array (genes)	Cells	RX (time in hours)	Common genes	Reference
cDNA, 7267	HUVEC	VEGF (0.5,2,6,12,24)	C8FW, DUSP5, EGR1, EGR2, NR4A1, VARS2	[41]
cDNA, 2400	HUVEC	LPS (4)	ATF3	[42]
cDNA, 7075	HAEC, CASmMC	TNF- $\alpha$ , IL-1B (24)	ICAM-1, TIEG	[43]
cDNA, 1185	HAEC	Shear stress (24)	Jun-B	[13]
cDNA, 9184	HMVEC	Trans RA, IFN- $\alpha$ , DI-TSP, TNP-470, Endo, PEDF (4)	No common genes	[44]
cDNA, 18,000	HUVEC	Shear stress (24)	EGR1, ICAM1	[45]
cDNA, 300	HUVEC	TNF- $\alpha$ , IL-1B (2,6,24)	EGR1, ICAM1	[45]
Affi., 12,600	PBMC	SU5416	No common genes	[46]
cDNA, 5000	VSMCs	Mechanical strain (12,24)	No common genes	[47]
Affi., 12,000	HUVEC	Egr-1 (1)	ATF3, ID2	[48]
Affi., 10,000	HUVEC	IFN- $\alpha$ A (0,5,12)	ICAM1	[49]
cDNA, 1024	HUVEC	Demethoxycurcumin (24)	No common genes	[50]
cDNA, 4000	HUVEC	Shear stress (6,24)	DOC1	[28]
Oligo, 35,000	HUVEC	TNF- $\alpha$ (2,4,6)	EDN1, ICAM1, Jun-B,	[51]
Oligo, 7000	HUVEC	ALK-1 and ALK-5 (TGF- $\beta$ receptors)	ICAM-1, ID1, ID2,	[52]
cDNA, 5000	MMECs	VEGF (3,6,12)	NR4A1	[53]
cDNA, 75000	HDMVEC	Endostatin (4)	FOS, JUN, ICAM1, ID1,	[24]
cDNA, 4000	HUVEC	LPS (1,4,7,12,24), TNF- $\alpha$ , IL-1B (1,4,7,12,24)	EDN1, FOSL1, JUN, PTGS2, RNASE1, TNFAIP3	[54,55]

The table summarizes published reports of microarray analysis of endothelial cells stimulated with various agents. It also gives a list of the genes that were common between these published reports and the present study. VSMCs, vascular smooth muscle cells; HAES, human coronary artery endothelial cells; HUVEC, human umbilical vein endothelial cells; HDMVEC, human dermal microvascular endothelial cells; CASmMC, human coronary artery smooth muscle cells; LPS, lipopolysaccharide; TNF $\alpha$ , tumor necrosis factor alpha.

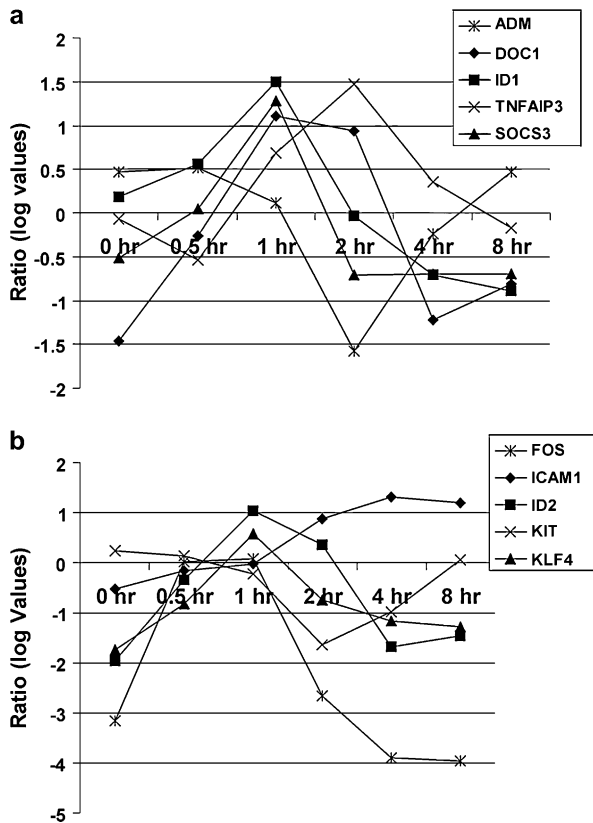


Fig. 3. The time course of the gene expression pattern. The line graphs of signals from microarray analysis of HUVEC treated with EMAP-II. The log<sub>2</sub> ratio of Cy5/Cy3 signal intensities are plotted against the different treatment intervals (0 h, 0.5 h, 1 h, 2 h, 4 h and 8 h). (a) The expression pattern for ADM, DOC1, ID1, TNFAIP3 and SOCS3 genes; (b) the patterns for FOS, ICAM1, ID2, KIT and KLF4.

reported in different studies to be modulated following EC activation by other cytokines. A composite list of published studies and genes common to the current study is shown (Table 2). We also observed a number of gene changes specific for EMAP-II stimulation that have not been previously reported. The genes involved have various functions including cell cycle arrest, apoptosis, cell proliferation and differentiation, vascular responses, and transcription regulation.

To validate the gene changes by real time RT-PCR, we selected 10 different genes from the 69 genes showed <0.5 and >2 fold changes on MA analysis. The genes were selected depending on their function and the magnitude of change observed on MA analysis. Their expression patterns showed either downregulation or moderate to high upregulation.

Our results demonstrated downregulation of the FOS and KIT oncogenes. FOS gene along with JUN has been implicated in cell growth, however, an important novel function for FosB dimerized with c-Jun, has been recently implicated in cell apoptosis [17]. KIT, a transmembrane glycoprotein, belongs to a receptor tyrosine kinase family and is implicated in the pathophysiology of a number of tumors [18]. The antiangiogenic

inhibitors, SU6668 and SU5416, inhibit biologic functions of c-kit in addition to exhibiting antiangiogenic properties [19]. Thus, downregulation of the KIT oncogene by EMAP-II indicates similar functions for EMAP-II.

The inhibitor of differentiation/DNA binding (Id) family of proteins are a helix-loop-helix (HLH) protein family implicated in a variety of cellular processes, including cellular growth, senescence, differentiation, apoptosis, angiogenesis and neoplastic transformation [20]. Id2, binds to the retinoblastoma protein to block cell cycle progression and also inhibits cell differentiation [21]. Although, EMAP-II upregulates ID1 and ID2 gene expression in HUVEC, the role of the ID genes in the EMAP-II induced HUVEC response is not known and will require further study.

ICAM-1 was upregulated in HUVEC following EMAP-II treatment. ICAM-1 is constitutively expressed at low levels on resting ECs, but is rapidly upregulated during inflammation, resulting in increased leukocyte/EC adhesion [22]. Clarijs et al. observed ICAM-1 immunostaining on the vascular endothelium in primary uveal melanomas with intense ubiquitous staining for EMAP-II, suggesting that EMAP-II binding to EC leads to ICAM-1 expression [23]. Our results showing upregulation of ICAM1 in ECs following EMAP-II treatment support this observation. Published reports show that the upregulation of ICAM-1 is a common event in HUVEC following stimulation with various agents (Table 2). Thus, EMAP-II might facilitate the process of chemotaxis through upregulation of ICAM-1 on vascular EC, which leads to localized vascular damage [23]. The recent report has shown downregulation of ICAM-1 after treating ECs with endostatin [24]. The difference might be because of different agent studied, as our work using endostatin modulated gene expression changes in HUVEC did not show upregulation of ICAM-1 [25].

The important feature of this study is to examine if there is any correlation among these 10 genes with respect to their expression changes in HUVEC following EMAP-II treatment. We wanted to examine if any one gene among these 10 genes modulated the expression of the remaining genes. To answer this question we decided to study the downregulated in ovarian cancer (DOC1) gene. The rationale to study DOC1 was because we observed upregulation of DOC1 in HUVEC stimulated with other antiangiogenic agents, endostatin and fumagillin as well [25]. Thus, DOC1 may serve as a common response gene in ECs following exposure with a variety of angiogenesis inhibitors. DOC1 was identified as a differentially expressed gene in human ovarian carcinoma by a DNA-fingerprinting approach. It has homology to mouse myosin heavy chain smooth muscle isoform (UniGene Sp: O08638) and myosin is an important cytoskeleton associated protein. A novel

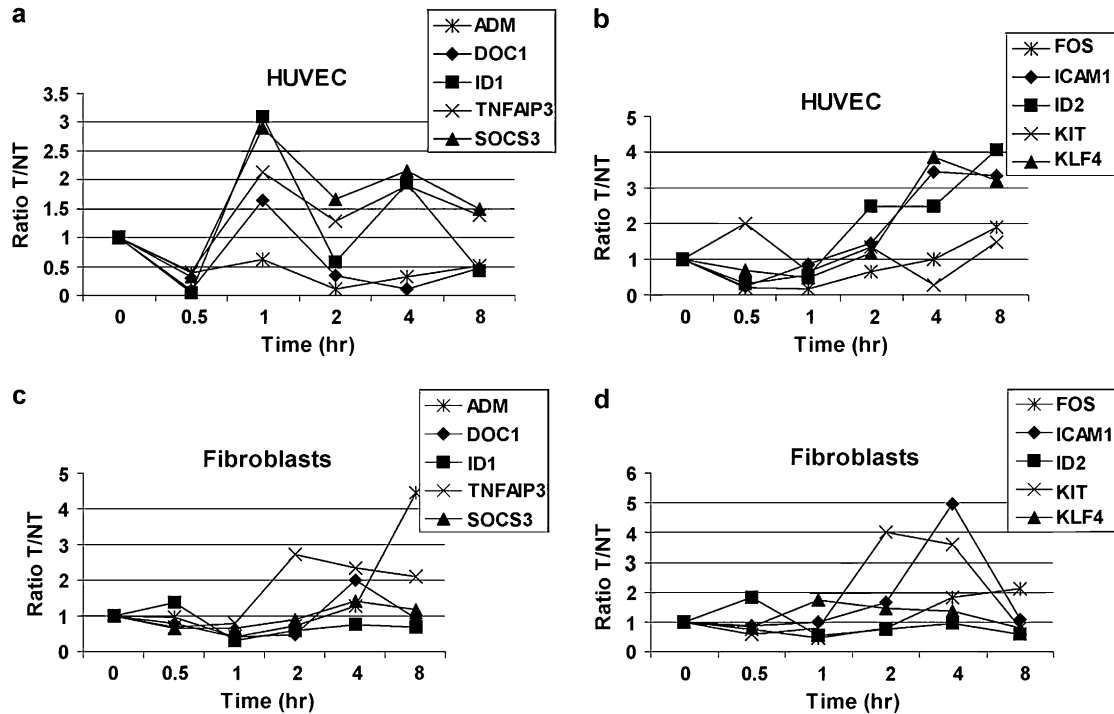


Fig. 4. Profile of EMAP-II stimulated changes in gene expression in HUVEC (a and b) and human fibroblasts (c and d). Total cellular RNA was extracted from cells treated with EMAP-II for 0 h, 0.5 h, 1 h, 2 h, 4 h and 8 h and subjected to real time RT-PCR. The ratio of EMAP-II treated/non-treated and standardized to GAPDH as an internal control is plotted against time. (a and c) The changes in transcript levels for genes ADM, DOC1, ID1, SOCS3, TNFAIP3 in HUVEC and fibroblasts, respectively; (b and d) the changes in transcript levels for the genes FOS, ICAM1, ID2, KIT and KLF4 in HUVEC and fibroblasts, respectively.

function in cellular senescence has been attributed to DOC1 recently [26]. Recent work by our group has shown that EMAP-II targets the EC cytoskeleton and the EMAP-II treated cells were in a less migratory state [15]. Cytoskeleton remodeling is crucial in many cellular events, including cell adhesion, spreading and motility and all these processes are required for angiogenesis [15]. Although not much is known about DOC1, it has been reported that DOC1 is present in normal ovarian surface epithelial cells but consistently absent in all of the ovarian cancer cell lines tested [27]. DOC1 has been shown to be upregulated in HUVEC subjected to shear stress [28]. Our results showed > 5 fold upregulation of DOC1 up to 2 h following exposure to EMAP-II.

To study if the inhibition of DOC1 could affect the levels of gene expression of other genes, we inhibited DOC1 expression using DOC1 specific SiRNA. We were able to demonstrate silencing of the DOC1 gene in HUVEC following EMAP-II exposure by DOC1 specific SiRNA. The silencing is specific to DOC1 SiRNA as we observed upregulation of DOC1 in scramble SiRNA treated HUVEC. Further, we checked levels of nine other genes in DOC1 SiRNA treated and EMAP-II stimulated HUVEC by real time RT-PCR. The silencing of the DOC1 gene reversed the stimulatory effect of EMAP-II on ADM, KLF4, SOCS3 and TNFAIP3 gene expression. Again the reversal effect

was specific to DOC1 SiRNA treatment; as scramble SiRNA treated HUVEC showed no effect of SiRNA treatment as such.

Among these genes, adrenomedullin (ADM) promotes proliferation and migration of ECs and is required for vascular morphogenesis [29,30]. It modulates EC function by activating the PI3K/Akt pathway in vascular ECs [31]. EMAP-II downregulated expression of ADM gene, however silencing of DOC1 inhibited EMAP-II induced downregulation of ADM. DOC1 SiRNA also inhibited the EMAP-II stimulated upregulation of Kruppel-like factor 4 (KLF4) in HUVEC. KLFs are key transcriptional regulators of cell proliferation, differentiation [32]. KLF4 directly transactivates p21, interacts with p53 and induces growth arrest and apoptosis [33–35]. Given the role of p53 in antiangiogenesis, it might be possible that p53 mediated suppression of angiogenesis involves EMAP-II and KLF4 [36].

There was a transient upregulation of TNF- $\alpha$  inducible early response gene (TNFAIP3). TNFAIP3 is involved in cell cycle arrest, apoptosis and it inhibits EC activation through a NF- $\kappa$ B dependent mechanism [37]. The other gene whose upregulation was inhibited by DOC1 SiRNA was suppressor of cytokine signaling 3 (SOCS3). The SOCS family of proteins has been implicated in the negative regulation of signal transduction by a variety of cytokines and are involved in

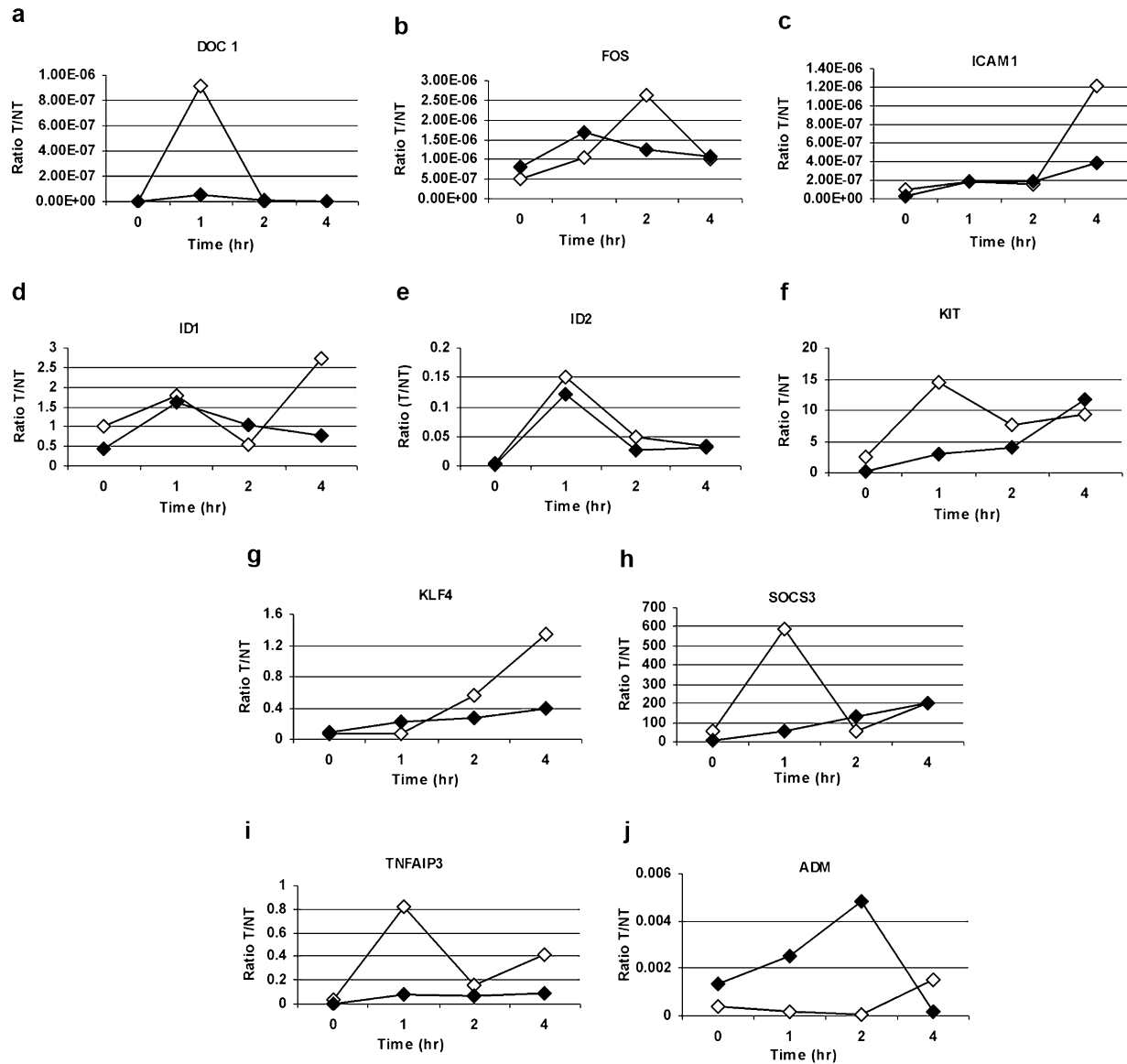


Fig. 5. Profile of EMAP-II stimulated changes in gene expression in HUVEC treated with control SiRNA (◇) and DOC1 SiRNA (◆). Total cellular RNA was extracted from HUVEC transfected with SiRNA and stimulated with EMAP-II for 0 h, 1 h, 2 h and 4 h and subjected to real time RT-PCR. DOC1 SiRNA abrogated EMAP-II stimulated DOC1 gene expression (a). Silencing of the DOC1 gene reversed the effects of EMAP-II on ADM (j), KLF4 (g), SOCS3 (h) and TNFAIP3 (i) gene expression with little effect on FOS (b), ICAM1 (c), ID1 (d) and KIT (f) genes and no effect on ID2 (e) gene expression.

proteasome-mediated degradation of proteins [38]. Since it is known that EMAP-II acts as a chemoattractant during the inflammatory response, the upregulation of SOCS3 by EMAP-II might play a role in removing unnecessary proteins resulting from inflammation.

Thus, our results demonstrate that, EMAP-II upregulates DOC1 in HUVEC, which in turn may modulate ADM, KLF4, SOCS3 and TNFAIP3. It is very tempting to hypothesize that these genes may be regulated by DOC1 and are downstream of DOC1 in the EMAP-II activation pathway. However, further work is needed to explore this possibility and to identify the downstream signaling stimulated by EMAP-II specifically in ECs.

Currently we are in the process of studying role of DOC1 in ECs. The identification of such a control pathway may lead to a better understanding of potential mechanisms that effect EC proliferation and can be used as targets for novel anti-cancer strategies.

## 4. Materials and methods

### 4.1. Cell culture

HUVEC were obtained from Biowhittaker/Cambrex and cultured in endothelial cell growth medium-2



supplemented with: 2% FBS, hydrocortisone, human fibroblast growth factor- $\beta$ , vascular endothelial growth factor, R3-insulin growth factor, ascorbic acid, human epidermal growth factor, GA-1000, and heparin (Clo-netics). Cell cultures were maintained in a humidified 95% air–5% CO<sub>2</sub> incubator at 37 °C. All experiments were conducted with HUVEC in passage 3. Human fibroblasts were grown in Dulbecco's modified Eagle's medium with 10% serum, 2 mM glutamine, 100  $\mu$ l/ml penicillin, 100  $\mu$ g/ml streptomycin, 100  $\mu$ g/ml gentamicin and fungizone.

#### 4.2. Production and purification of EMAP-II protein

DH5 $\alpha$  cells transformed with the pET-20b plasmid, expressing mature EMAP-II as a histidine tagged protein, were obtained from Paul Schimmel at The Scripps Research Institute, La Jolla, CA. The bacterial cultures were induced with isopropyl- $\beta$ -D-thiogalactoside (Sigma) and lysed by lysis buffer (50 mM Tris–HCl pH 7.5, 0.15 M NaCl, 10% sucrose) containing 200  $\mu$ g/ml lysozyme on ice for 30 min. Triton X-100 was added at a final concentration of 1% and incubated at 4 °C for 30 min. The samples were centrifuged at 15,000 rpm for 30 min. The supernatants were incubated with Ni-NTA Superflow affinity resin (Qiagen; 1 ml bed volume per 100 ml supernatant) for 1 h at 4 °C. The fusion protein was eluted from the affinity column using elution buffer (20 mM Tris–HCl pH 7.9, 0.25 M NaCl, 10% glycerol) containing different concentrations (10 mM, 50 mM, 100 mM and 200 mM) of imidazole (Fisher Biotech). The different fractions were checked for the presence of biologically active EMAP-II using a tissue factor assay as previously described [10]. EMAP-II was eluted at 100 mM imidazole concentration. Protein concentrations were checked by BCA protein assay kit (Pierce) and the purity of the proteins was confirmed by electrophoresis on 10% NuPAGE Bis-Tris gels (Invitrogen).

#### 4.3. EMAP-II treatment

Prior to treatment, HUVEC and human fibroblasts were plated in 6-well plates containing  $0.5 \times 10^6$  cells per well. After 24 h of growth, when cells were 70–80% confluent, they were treated with 10  $\mu$ g/ml of EMAP-II for 0 h, 0.5 h, 1 h, 2 h, 4 h and 8 h. Controls were treated in a similar way with the elution buffer used to purify EMAP-II. After incubation cells were washed with PBS and used either for cDNA MA analysis or real time RT-PCR.

#### 4.4. Cell proliferation assay

A colorimetric assay for the quantification of cell proliferation and cell viability, based on the cleavage of the tetrazolium salt WST-1 by mitochondrial dehydro-

genase in viable cells was performed according to the manufacturer's instructions (Roche Molecular Biochemicals, Germany). Briefly,  $2 \times 10^3$  HUVEC or human fibroblast cells were plated in 96-well microtiter plates to a final volume of 100  $\mu$ l/well. After 24 h, cells were treated with EMAP-II (10  $\mu$ g/ml) for 2 h, 4 h, 1 day, 3 days and 5 days. After the treatment, 10  $\mu$ l/well of WST-1 reagent was added and cells were further incubated at 37°C for 4 h. The absorbance of the samples was measured at 440 nm with 600 nm as a reference wavelength using a microtiter plate reader (Benchmark Microplate Reader, BIO-RAD). Cells treated with EMAP-II elution buffer and 10  $\mu$ g/ml of endostatin was used as negative and positive controls respectively. The cytotoxic agent, 5-FU (50  $\mu$ g/ml) (Sigma Aldrich) was used as a positive control for fibroblasts proliferation inhibition.

#### 4.5. Preparation of cDNA

Total RNA was isolated from cells using the RNeasy total RNA kit (Qiagen, Germany) according to the manufacturer's protocol. The extracted total RNA was amplified to produce enhanced quantities of antisense RNA for subsequent hybridizations [39,40]. Briefly, 3  $\mu$ g of total RNA was converted to cDNA using the T7 primer and subsequently converted back to RNA using a T7 Megascript kit (Ambion Inc., USA). Further, 3  $\mu$ g of amplified RNA was converted into sense cDNA using Superscript II reverse transcriptase and aminoallyl-dUTP. The cDNA was column purified using QIAquick PCR purification kit (Qiagen, Germany). For the forward array, the control (untreated cells) cDNA was coupled with Cy5 dye and the test RNA (treated cells) was coupled with Cy3 dye and for the reverse array the dyes were switched to control for labeling bias. The uncoupled dye was removed using QIAquick Nucleotide Removal kit (Qiagen, Germany). Human 10K cDNA array slides (NCI-ATC Microarray facility, Gaithersburg, MD) were prehybridized for 45 min at 42 °C. The control and test cDNA were mixed together with 20  $\mu$ g of human Cot1-DNA, 20  $\mu$ g of Poly(A)-DNA and 1  $\mu$ l of yeast tRNA to block nonspecific hybridization, denatured at 95 °C for 3 min and hybridized to 10K UniGEM V cDNA arrays (NCI Array Facility) in 50% formamide,  $5 \times$  SSC and 0.1% SDS hybridization buffer at 42 °C for 16–20 h.

#### 4.6. Microarray image acquisition and data analysis

The slides were washed in three consecutive washes of decreasing ionic strengths. Microarrays were scanned in both Cy3 and Cy5 channels using a GenePix Personal 4100 A scanner (Axon Instruments, California). The background was determined from the intensity reading around the spotted areas and subtracted from the

reading of the spot. The normalized results were used to calculate the ratio for each gene. The analysis was done by uploading array images and the gene ratios on the NCI microarray website (<http://nciarray.nci.nih.gov>). The data was retrieved into Microsoft (MS) Excel spreadsheets to draw the line graphs.

The scatter plots were drawn by loading MS Excel data into BRB-Array tools version 3.0.2 (<http://linus.nci.nih.gov/BRB-ArrayTools.html>).

#### 4.7. Quantitative real time RT-PCR

First strand cDNAs were generated from the total RNA. Quantitative RT-PCR was performed using a Gene Amp 5700 Sequence Detector (Applied Biosystems). The amount of the PCR product was measured as fluorescent signal intensity after standardizing to human GAPDH internal control, which is proportional to the amount of target gene present in the sample.

The following sense (S) and antisense (AS) primers and probes were designed using Primer Express 2.0 software (Applied Biosystems) for real time RT-PCR analysis

#### ADM

S 5' CCGTCGCCCTGATGTACCT 3'  
AS 5' GAGCCCACTTATTCCACTTCTTTC 3'  
Probe 5' CGCTCGGTTGGATGTGCGGTC 3'

#### DOC1

S 5' AGTCCATACTGATATTTTTGCAAGGA-A 3'  
AS 5' CCCAAAGTACGAGTTCAGTCAGTCT 3'  
Probe 5' ATCCTTTTTTAATCATCCCTCCATATC-CCCC 3'

#### FOS

S 5' CCCAAGCCCTCAGTGGAA 3'  
AS 5' ACTGGGCCTGGATGATGCT 3'  
Probe 5' AGACCGAGCCCTTTGATGACTTCCT-GTTC 3'

#### ICAM1

S 5' GGCTGACGTGTGCAGTAATACTG 3'  
AS 5' CGCCGGAAAGCTGTAGATG 3'  
Probe 5' AACCAGAGCCAGGAGACACTGCAG-ACA 3'

#### ID1

S 5' AGAACCGCAAGGTGAGCAA 3'  
AS 5' CCAACTGAAGGTCCCTGATGTA  
Probe 5' TGGAGATTCTCCAGCACGTCATCGAC 3'

#### ID2

S 5' TGGACTCGCATCCCACTATTG 3'  
AS 5' GTCCTGGACGCCTGGTTCT 3'  
Probe 5' CAGCCTGCATCACCAGAGACCCG 3'

#### KIT

S 5' CGAGTGCCCATTTGACAGAA 3'  
AS 5' GCAGGCTCCAAGTAGATTCA 3'  
Probe 5' AAGCCCTCATGTCTGAACTCAAAGT-CCTGA 3'

#### KLF4

S 5' ACCAGGCACTACCGTAAACACA 3'  
AS 5' GGTCCGACCTGGAAAATGCT 3'  
Probe 5' CCGTTCCAGTGCCAAAAATGCGA 3'

#### SOCS3

S 5' CCCCAGAAGAGCCTATTACATCTAC-T3'  
AS 5' TTCCGACAGAGATGCTGAAGAGT 3'  
Probe 5' CCCCTGGTGTTGAGCCGGC 3'

#### TNFAIP3

S 5' GGAAGCACCATGTTTGAAGGATA 3'  
AS 5' GCTCGATCTCAGTTGCTCTTCTG 3'  
Probe 5' AAGCTCAGAATCAGAGATTTTCATGA-GGCCA 3'

#### 4.8. Gene silencing by SiRNA

We selected the DOC1 gene to further study its role in EMAP-II stimulated HUVEC gene expression using a pSiRNA system developed by Invivogen (San Diego). Four 19-nucleotide (nt) dsDNA sequences complementary to DOC1 mRNA were cloned into a RNA polymerase III based expression vector (pSiRNA-Neo) that enabled the endogenous production of small dsRNAs targeting the DOC1 gene. Among the four SiRNA synthesized for the DOC1 gene, we used the sequence that gave the least number of hits after a BLAST (<http://www.ncbi.nlm.nih.gov/BLAST>) search. Vector containing a null sequence (intron1 repeat polymorphism of the human tyrosine hydroxylase gene) was created as a control. The 19nt sequences cloned into the 2.5 kb expression vectors are:

pSiRNA-Neo-DOC1: 5' AGCGTAACCAAGGA-GAGAGAT3' (accession number [XM\\_002964](#), position 1172–1192)

pSiRNA-Neo-Control: 5' ATTCATTCATTCATT-CACCAT3' (accession number [D00269](#), position 1192–1212)

HUVEC were transfected using lipofectamine (Invitrogen) with 1 µg of either pSiRNA-Neo-DOC1 or pSiRNA-Neo-Control vectors expressing SiRNA for DOC1 or control genes respectively. After 48 h of transfection, cells were grown in the media containing neomycin analogue G418. The neomycin resistant clones were selected and grown further to use in the real time RT-PCR assays.

## References

- [1] Kao J, Ryan J, Brett G, Chen J, Shen H, Fan YG, et al. Endothelial monocyte-activating polypeptide II. A novel tumor-derived polypeptide that activates host-response mechanisms. *J Biol Chem* 1992;267:20239–47.
- [2] Kao J, Houck K, Fan Y, Haehnel I, Libutti SK, Kayton ML, et al. Characterization of a novel tumor-derived cytokine. Endothelial-monocyte activating polypeptide II. *J Biol Chem* 1994;269:25106–19.
- [3] Behrendorf HA, van de Craen M, Knies UE, Vandenabeele P, Clauss M. The endothelial monocyte-activating polypeptide II (EMAP II) is a substrate for caspase-7. *FEBS Lett* 2000;466:143–7.
- [4] Barnett G, Jakobsen AM, Tas M, Rice K, Carmichael J, Murray JC. Prostate adenocarcinoma cells release the novel proinflammatory polypeptide EMAP-II in response to stress. *Cancer Res* 2000;60:2850–7.
- [5] Chang SY, Park SG, Kim S, Kang CY. Interaction of the C-terminal domain of p43 and the alpha subunit of ATP synthase. Its functional implication in endothelial cell proliferation. *J Biol Chem* 2002;277:8388–94.
- [6] Schwarz MA, Kandel J, Brett J, Li J, Hayward J, Schwarz RE, et al. Endothelial-monocyte activating polypeptide II, a novel antitumor cytokine that suppresses primary and metastatic tumor growth and induces apoptosis in growing endothelial cells. *J Exp Med* 1999;190:341–54.
- [7] Berger AC, Alexander HR, Wu PC, Tang G, Gnant MF, Mixon A, et al. Tumour necrosis factor receptor I (p55) is upregulated on endothelial cells by exposure to the tumour-derived cytokine endothelial monocyte-activating polypeptide II (EMAP-II). *Cytokine* 2000;12:992–1000.
- [8] Zhang FR, Schwarz MA. Pro-EMAP II is not primarily cleaved by caspase-3 and -7. *Am J Physiol Lung Cell Mol Physiol* 2002;282:L1239–44.
- [9] Wu PC, Alexander HR, Huang J, Hwu P, Gnant M, Berger AC, et al. In vivo sensitivity of human melanoma to tumor necrosis factor (TNF)-alpha is determined by tumor production of the novel cytokine endothelial-monocyte activating polypeptide II (EMAPII). *Cancer Res* 1999;59:205–12.
- [10] Gnant MF, Berger AC, Huang J, Puhlmann M, Wu PC, Merino MJ, et al. Sensitization of tumor necrosis factor alpha-resistant human melanoma by tumor-specific in vivo transfer of the gene encoding endothelial monocyte-activating polypeptide II using recombinant vaccinia virus. *Cancer Res* 1999;59:4668–74.
- [11] Schena M, Shalon D, Davis RW, Brown PO. Quantitative monitoring of gene expression patterns with a complementary DNA microarray. *Science* 1995;270:467–70.
- [12] Shalon D, Smith SJ, Brown PO. A DNA microarray system for analyzing complex DNA samples using two-color fluorescent probe hybridization. *Genome Res* 1996;6:639–45.
- [13] Chen BP, Li YS, Zhao Y, Chen KD, Li S, Lao J, et al. DNA microarray analysis of gene expression in endothelial cells in response to 24-h shear stress. *Physiol Genomics* 2001;7:55–63.
- [14] Bassett Jr DE, Eisen MB, Boguski MS. Gene expression informatics—it's all in your mine. *Nat Genet* 1999;21:51–5.
- [15] Keezer SM, Ivie SE, Krutzsch HC, Tandle A, Libutti SK, Roberts DD. Angiogenesis inhibitors target the endothelial cell cytoskeleton through altered regulation of heat shock protein 27 and cofilin. *Cancer Res* 2003;63:6405–12.
- [16] Chua MS, Sarwal MM. Microarrays: new tools for transplantation research. *Pediatr Nephrol* 2003;18:319–27.
- [17] Baumann S, Hess J, Eichhorst ST, Krueger A, Angel P, Krammer PH, et al. An unexpected role for FosB in activation-induced cell death of T cells. *Oncogene* 2003;22:1333–9.
- [18] Heinrich MC, Blanke CD, Druker BJ, Corless CL. Inhibition of KIT tyrosine kinase activity: a novel molecular approach to the treatment of KIT-positive malignancies. *J Clin Oncol* 2002;20:1692–703.
- [19] Smolich BD, Yuen HA, West KA, Giles FJ, Albitar M, Cherrington JM. The antiangiogenic protein kinase inhibitors SU5416 and SU6668 inhibit the SCF receptor (c-kit) in a human myeloid leukemia cell line and in acute myeloid leukemia blasts. *Blood* 2001;97:1413–21.
- [20] Ruzinova MB, Benezra R. Id proteins in development, cell cycle and cancer. *Trends Cell Biol* 2003;13:410–8.
- [21] Lasorella A, Iavarone A, Israel MA. Id2 specifically alters regulation of the cell cycle by tumor suppressor proteins. *Mol Cell Biol* 1996;16:2570–8.
- [22] Dustin ML, Rothlein R, Bhan AK, Dinarello CA, Springer TA. Induction by IL 1 and interferon-gamma: tissue distribution, biochemistry, and function of a natural adherence molecule (ICAM-1). *J Immunol* 1986;137:245–54.
- [23] Clarijs R, Schalkwijk L, Ruiters DJ, de Waal RM. EMAP-II expression is associated with macrophage accumulation in primary uveal melanoma. *Invest Ophthalmol Vis Sci* 2003;44:1801–6.
- [24] Abdollahi A, Hahnfeldt P, Maercker C, Grone HJ, Debus J, Ansgor W, et al. Endostatin's antiangiogenic signaling network. *Mol Cell* 2004;13:649–63.
- [25] Mazzanti CM, Tandle A, Lorang D, Costouros N, Roberts D, Bevilacqua G, et al. Early genetic mechanisms underlying the inhibitory effects of endostatin and fumagillin on human endothelial cells. *Genome Res* 2004;14:1585–93.
- [26] Schwarze SR, DePrimo SE, Grabert LM, Fu VX, Brooks JD, Jarrard DF. Novel pathways associated with bypassing cellular senescence in human prostate epithelial cells. *J Biol Chem* 2002;277:14877–83.
- [27] Mok SC, Wong KK, Chan RK, Lau CC, Tsao SW, Knapp RC, et al. Molecular cloning of differentially expressed genes in human epithelial ovarian cancer. *Gynecol Oncol* 1994;52:247–52.
- [28] McCormick SM, Eskin SG, McIntire LV, Teng CL, Lu CM, Russell CG, et al. DNA microarray reveals changes in gene expression of shear stressed human umbilical vein endothelial cells. *Proc Natl Acad Sci U S A* 2001;98:8955–60.
- [29] Imai Y, Shiindo T, Maemura K, Kurihara Y, Nagai R, Kurihara H. Evidence for the physiological and pathological roles of adrenomedullin from genetic engineering in mice. *Ann N Y Acad Sci* 2001;947(26-33):33–4.
- [30] Miyashita K, Itoh H, Sawada N, Fukunaga Y, Sone M, Yamahara K, et al. Adrenomedullin promotes proliferation and migration of cultured endothelial cells. *Hypertens Res* 2003;26:S93–8.
- [31] Nishimatsu H, Suzuki E, Nagata D, Moriyama N, Satonaka H, Walsh K, et al. Adrenomedullin induces endothelium-dependent vasorelaxation via the phosphatidylinositol 3-kinase/Akt-dependent pathway in rat aorta. *Circ Res* 2001;89:63–70.
- [32] Bieker JJ. Kruppel-like factors: three fingers in many pies. *J Biol Chem* 2001;276:34355–8.
- [33] Zhang W, Geiman DE, Shields JM, Dang DT, Mahatan CS, Kaestner KH, et al. The gut-enriched Kruppel-like factor (Kruppel-like factor 4) mediates the transactivating effect of p53 on the p21WAF1/Cip1 promoter. *J Biol Chem* 2000;275:18391–8.
- [34] Yoon HS, Chen X, Yang VW. Kruppel-like factor 4 mediates p53-dependent G1/S cell cycle arrest in response to DNA damage. *J Biol Chem* 2003;278:2101–5.
- [35] Ohnishi S, Ohnami S, Laub F, Aoki K, Suzuki K, Kanai Y, et al. Downregulation and growth inhibitory effect of epithelial-type Kruppel-like transcription factor KLF4, but not KLF5, in bladder cancer. *Biochem Biophys Res Commun* 2003;308:251–6.
- [36] Van Meir EG, Polverini PJ, Chazin VR, Su Huang HJ, de Tribolet N, Cavenee WK. Release of an inhibitor of angiogenesis upon induction of wild type p53 expression in glioblastoma cells. *Nat Genet* 1994;8:171–6.

- [37] Cooper JT, Stroka DM, Brostjan C, Palmethofer A, Bach FH, Ferran C. A20 blocks endothelial cell activation through a NF-kappaB-dependent mechanism. *J Biol Chem* 1996;271:18068–73.
- [38] Kile BT, Schulman BA, Alexander WS, Nicola NA, Martin HM, Hilton DJ. The SOCS box: a tale of destruction and degradation. *Trends Biochem Sci* 2002;27:235–41.
- [39] Phillips J, Eberwine JH. Antisense RNA amplification: a linear amplification method for analyzing the mRNA population from single living cells. *Methods* 1996;10:283–8.
- [40] Wang E, Miller LD, Ohnmacht GA, Liu ET, Marincola FM. High-fidelity mRNA amplification for gene profiling. *Nat Biotechnol* 2000;18:457–9.
- [41] Abe M, Sato Y. cDNA microarray analysis of the gene expression profile of VEGF-activated human umbilical vein endothelial cells. *Angiogenesis* 2001;4:289–98.
- [42] Ahn SK, Choe TB, Kwon TJ. The gene expression profile of human umbilical vein endothelial cells stimulated with lipopolysaccharide using cDNA microarray analysis. *Int J Mol Med* 2003;12:231–6.
- [43] Bandman O, Coleman RT, Loring JF, Seilhamer JJ, Cocks BG. Complexity of inflammatory responses in endothelial cells and vascular smooth muscle cells determined by microarray analysis. *Ann N Y Acad Sci* 2002;975:77–90.
- [44] Cline EI, Biciato S, DiBello C, Lingen MW. Prediction of in vivo synergistic activity of antiangiogenic compounds by gene expression profiling. *Cancer Res* 2002;62:7143–8.
- [45] Dekker RJ, van Soest S, Fontijn RD, Salamanca S, de Groot PG, VanBavel E, et al. Prolonged fluid shear stress induces a distinct set of endothelial cell genes, most specifically lung Kruppel-like factor (KLF2). *Blood* 2002;100:1689–98.
- [46] DePrimo SE, Wong LM, Khatry DB, Nicholas SL, Manning WC, Smolich BD, et al. Expression profiling of blood samples from an SU5416 Phase III metastatic colorectal cancer clinical trial: a novel strategy for biomarker identification. *BMC Cancer* 2003;3:3.
- [47] Feng Y, Yang JH, Huang H, Kennedy SP, Turi TG, Thompson JF, et al. Transcriptional profile of mechanically induced genes in human vascular smooth muscle cells. *Circ Res* 1999;85:1118–23.
- [48] Fu M, Zhu X, Zhang J, Liang J, Lin Y, Zhao L, et al. Egr-1 target genes in human endothelial cells identified by microarray analysis. *Gene* 2003;315:33–41.
- [49] Gomez D, Reich NC. Stimulation of primary human endothelial cell proliferation by IFN. *J Immunol* 2003;170:5373–81.
- [50] Kim JH, Shim JS, Lee SK, Kim KW, Rha SY, Chung HC, et al. Microarray-based analysis of anti-angiogenic activity of demethoxycurcumin on human umbilical vein endothelial cells: crucial involvement of the down-regulation of matrix metalloproteinase. *Jpn J Cancer Res* 2002;93:1378–85.
- [51] Murakami T, Mataka C, Nagao C, Umetani M, Wada Y, Ishii M, et al. The gene expression profile of human umbilical vein endothelial cells stimulated by tumor necrosis factor alpha using DNA microarray analysis. *J Atheroscler Thromb* 2000;7:39–44.
- [52] Ota T, Fujii M, Sugizaki T, Ishii M, Miyazawa K, Aburatani H, et al. Targets of transcriptional regulation by two distinct type I receptors for transforming growth factor-beta in human umbilical vein endothelial cells. *J Cell Physiol* 2002;193:299–318.
- [53] Weston GC, Haviv I, Rogers PA. Microarray analysis of VEGF-responsive genes in myometrial endothelial cells. *Mol Hum Reprod* 2002;8:855–63.
- [54] Zhao B, Bowden RA, Stavchansky SA, Bowman PD. Human endothelial cell response to gram-negative lipopolysaccharide assessed with cDNA microarrays. *Am J Physiol Cell Physiol* 2001;281:C1587–95.
- [55] Zhao B, Stavchansky SA, Bowden RA, Bowman PD. Effect of interleukin-1beta and tumor necrosis factor-alpha on gene expression in human endothelial cells. *Am J Physiol Cell Physiol* 2003;284:C1577–83.